N O T I C E

THIS DOCUMENT HAS BEEN REPRODUCED FROM
MICROFICHE. ALTHOUGH IT IS RECOGNIZED THAT
CERTAIN PORTIONS ARE ILLEGIBLE, IT IS BEING RELEASED
IN THE INTEREST OF MAKING AVAILABLE AS MUCH
INFORMATION AS POSSIBLE

FINAL REPORT FOR CONTRACT NAS9-15887

COMPUTERIZED TOMOGRAPHIC DETERMINATION OF SPINAL BONE MINERAL CONTENT

Christopher E. Cann, Ph.D.

Harry K. Genant, M.D.

Department of Radiology

University of California

San Francisco, California 94143

TASK I. To improve the accuracy of vertebral mineral determination using
dual-energy CT techniques.

The Basis of Vertebral Mineral Estimation Using Computed Tomography

Computed tomography measures the CT number, H, which is related to the
total linear attenuation coefficient μ in any particular volume element. Most
scanners are calibrated on a scale such that H for water is 0 and H for air is
-1000 (Hounsfield scale). Thus, 1000 units represents the change in μ corresponding
to a density difference of 1.00 gm cm^{-3} for water. Vertebral bone mixture is a
combination of mineral, soft tissue and fat, and the measured CT number is derived
from a linear combination of the attenuation coefficients, densities and concentra-
tions of these components (Figure 1). For the vertebral bone mixture in a typical
older adult and an 80 kVp incident x-ray spectrum, about 26% of the total μ is
contributed by bone mineral--half due to the higher effective atomic number and
half due to the increased density of hydroxyapatite relative to water.

If one assumes that mineral lost between serial scans is replaced by water-
equivalent soft tissue, then the change in vertebral mineral can be estimated by
the change in that portion of the CT number due to the mineral fraction. For example,
a change in CT number of 50 units, from 300 to 250, would represent the same decrease
in μ that would be observed for a change in density of a material with the same μ
as water from 1.300 gm cm^{-3} to 1.250 gm cm^{-3}, or approximately 4%. If the non-mineral
fraction of the vertebra was water-equivalent soft tissue with a CT number of 0 then
the decrease in mineral would be 50/300 or 17%.

In serial studies, the inaccuracy introduced by assuming replacement of
bone by soft tissue and ignoring the fat content of the spinal bone mixture contri-
butes an error of only 0.1% to the precision of mineral measurement using single
energy CT. If the replacement tissue is fat, as is physiologically probable, rather
than soft tissue the additional error is 0.15%. In actuality, the non-mineral fraction
of the vertebral body contains varying concentrations of fat and its CT number will be
less than 0 (approximately 12 units per 10% fat by weight). This will contribute a
significant inaccuracy in the absolute determination of mineral since the true mineral-
dependent component of the CT number could be as much as 35 units higher than estimated
for a 30% fat content. Dual energy CT can reduce this inaccuracy (1). Precision
is less, however, because of positioning, motion and other errors between scans when
a patient is scanned at two energies (2). Thus, while dual energy CT is necessary
for diagnostic purposes where accuracy is important, single energy CT is most useful
for serial studies where high precision is necessary. Our in vivo precision for
vertebral mineral determination is currrntly 1.54% (coefficient of variation), and
these methods are used for the studies in Task 4.

Accuracy

Our experience in the last several years in developing CT for vertebral
mineral determination has identified many factors which affect the accuracy of this
method. The most important factors affecting the absolute accuracy of measured
mineral content are the accuracy of the calculated CT numbers generated by the
manufacturer's algorithm and the chemical composition of the vertebral bone mixture.

If an x-ray source used to produce a CT image were truly monoenergetic,
the calculated CT numbers would be accurate to the counting statistics used

FRACTION OF VERTEBRAL CANCELLOUS BONE MIXTURE OCCUPIED BY MINERAL, FAT AND SOFT TISSUE

SOFT TISSUE
FAT
BONE MINERAL

63

60

56

25

20

18

12

20

26

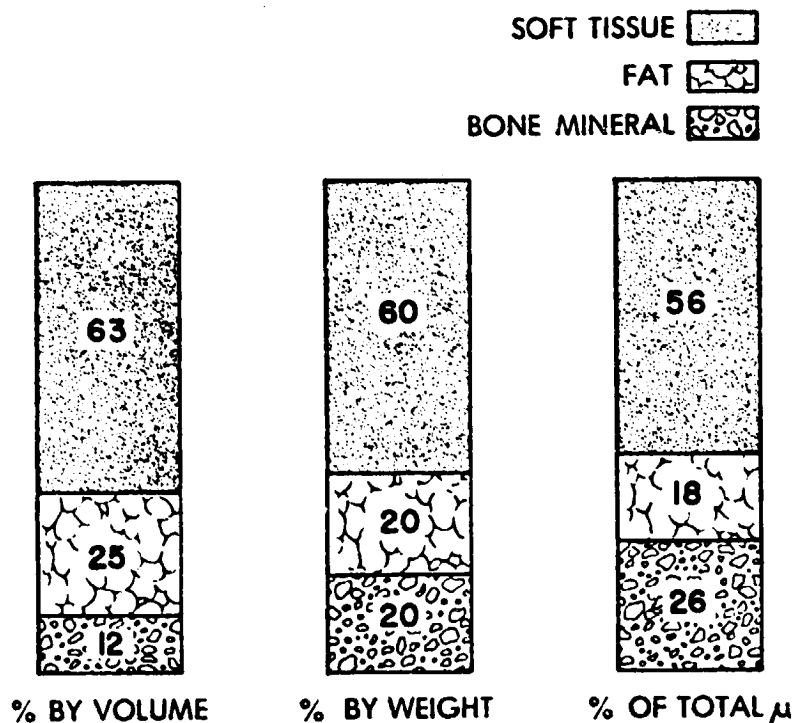% BY VOLUME   % BY WEIGHT   % OF TOTAL μ

Figure 1.   Composition of the vertebral cancellous bone mixture of a
typical older adult in terms of weight, volume and attenuation
coefficient.

(x-ray dose). Unfortunately x-ray sources are far from monoenergetic, and the polychromatic nature of the source causes significant inaccuracies in the calculated CT numbers. The main problem in this regard is beam-hardening, the preferential attenuation of the low energy x-rays present in the source spectrum. This effect is a non-linear function of object thickness, and complicated by the fact that it is also dependent upon the chemical composition of the object being scanned. Most scanners employ a correction to reduce the errors from this source. This single-energy preprocessing correction, however, is usually based on correction of the non-linear attenuation of x-ray transmission through a water phantom. As such, it is suboptimal as a correction for the human torso and does not address at all the presence of bone in the body. There are two methods to address the beam-hardening problem: 1) post-processing, or correction of the calculated display image, and 2) dual-energy pre-processing, or modification of the projection data to include the beam hardening effects. Post-processing has been tried by some manufacturers and has been shown to improve image quality. The basis for this correction, however, is adding a non-linear correction to an image generated using linear reconstruction methods, and this can introduce inaccuracies in the "corrected" CT numbers (3). The dual-energy pre-processing approach avoids this problem, but necessitates access to the raw projection data in order to modify the line integrals. We have elected to use this pre-processing approach to correct for beam hardening.

Our preliminary studies (1,2,4) addressed the possibility of dual energy CT bone mineral estimation to correct for the presence of variable fat in spinal bone mixture. The EMI head scanner was used at 80 and 140 kVp to measure coaxial phantoms containing solutions of dipotassium hydrogen phosphate, water and ethyl alcohol which simulate variable bone, soft tissue, and fat. The results indicated that the CT technique at a single energy can readily and accurately determine mineral content for cortical, cancellous or integral bone in a two component system containing mineral and soft tissue. In two component phantoms, it can do this with accuracy matching or surpassing the Norland-Cameron technique which can measure only integral bone. Additionally, in the dual energy mode (1), fat can be determined relatively accurately, albeit at a considerable sacrifice of precision.

For analysis of the axial skeleton, particularly the spine where complications of bone loss frequently become manifest additional sources of errors exist, yet the dual energy CT technique discussed herein may prove particularly valuable. Since CT uses relatively high photon energies for statistical and dosimetric reasons, the relative error due to marrow fat may be considerable, up to 35 HU in older populations. This suggests the necessity for dual energy technique for the thicker body parts.

Preliminary dual energy determinations in a phantom containing excised vertebrae were evaluated. Bone mineral content for the midportion of the vertebrae enclosed in the phantom was calculated from the dual energy data available from the serial scans performed on the phantom. The mean of 16 measurements at the same scan site was 74.6 mg/ml with a standard deviation of 10.8. These results confirmed the lower precision of dual energy CT bone mineral content determination previously obtained (1) and predicted by theory (2). The accuracy of the method for spine specimens and the reliability of patient data using the dual energy method were not determined.

The accuracy of single-energy CT scanning for vertebral mineral content in vivo was determined in a monkey (5) (Figure 2). Dispersion about the regression line was 5.5% for this two component system (fat content within these monkey vertebral bodies was negligible).

All of this preliminary work with dual-energy scanning was done with data obtained in standard reconstructed CT images. While these methods are useful, they are limited in two major ways; 1) by the accuracy of the CT numbers themselves and 2) by the inability to separate fully the contributions to x-ray attenuation from the mineral component and the soft tissue component. Commerical CT scanners normally produce an accurate water phantom scan for a single tube potential. Calibrations for scans done at other effective scan energies are not easily obtainable, and thus the CT numbers obtained in these scans are not accurate. For example, water is 50 HU at 80 kVp on our scanners and a water phantom has some cupping artifact. Thus, the "dual-energy" data obtained from two reconstructed images has an inherent inaccuracy.

To correct for these inaccuracies, we have adopted a dual-energy approach which uses the raw projection data from two different spectral distributions produced either by two tube potentials or selective filtration. The two sets of data are used to reconstruct energy-selective images of just the "mineral" component or the "soft-tissue" component (Figure 3). This approach also removes the beam-hardening inaccuracies due to the polychromatic nature of the x-ray spectrum.

METHODS: Energy selective reconstruction

a. Background

Chemical composition data produced from single-energy CT methods must assume a 2-component matrix which produces the observed CT numbers or attenuation values. This is obtained by solving the equations

$$\mu(E) = \frac{c_1}{\rho_1} \mu_1(E) + \frac{c_2}{\rho_2} \mu_2(E)$$

and
$$\frac{c_1}{\rho_1} + \frac{c_2}{\rho_2} = 1$$

When a third component of known attenuation but unknown concentration is introduced into the system, the determination of any of the 3 components is non-unique. If the attenuation coefficient of one of the 3 components varies significantly with energy, it can be distinguished from the others, a third equation can be produced and a unique solution found for chemical composition. This can be written

$$\mu(E_1) = \frac{c_1}{\rho_1} \mu_1(E_1) + \frac{c_2}{\rho_2} \mu_2(E_1) + \frac{c_3}{\rho_3} \mu_3(E_1)$$

$$\mu(E_2) = \frac{c_1}{\rho_1} \mu_1(E_2) + \frac{c_2}{\rho_2} \mu_2(E_2) + \frac{c_3}{\rho_3} \mu_3(E_2)$$

$$\frac{c_1}{\rho_1} + \frac{c_2}{\rho_2} + \frac{c_3}{\rho_3} = 1$$

where $\mu(E_1)$ and $\mu(E_2)$ are the effective attenuation coefficients of a volume containing a mixture of the three components.
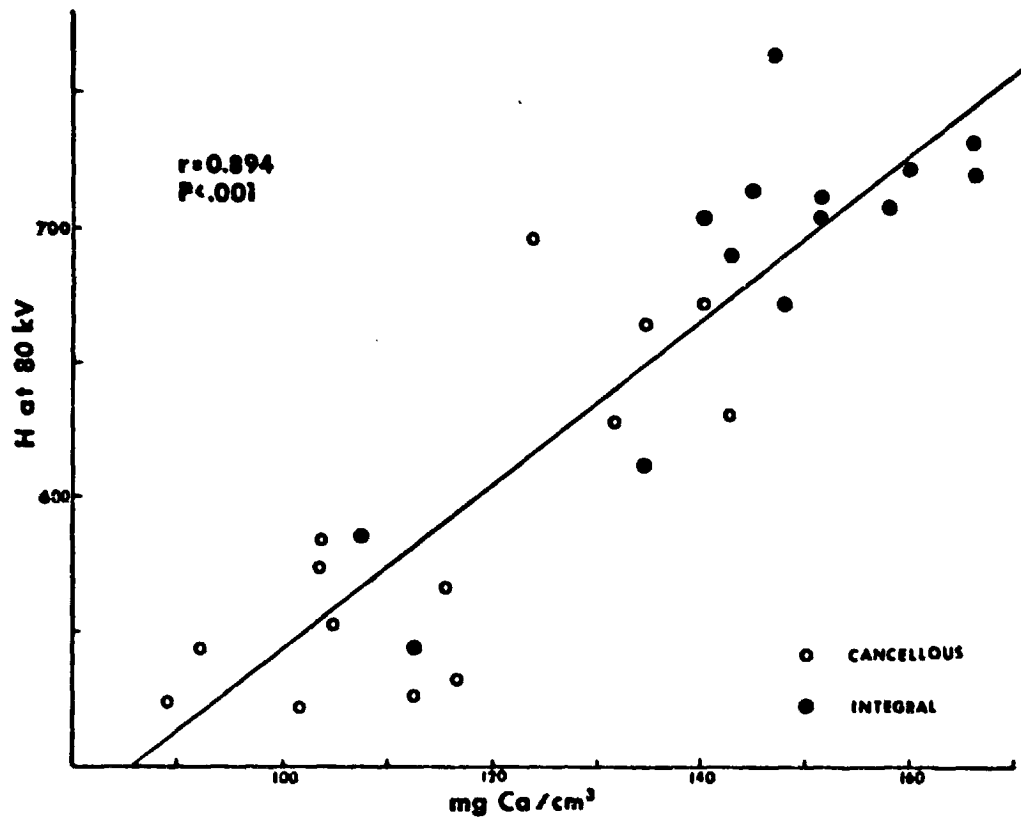
Figure 2.   Correlation between the CT number of monkey vertebrae in vivo
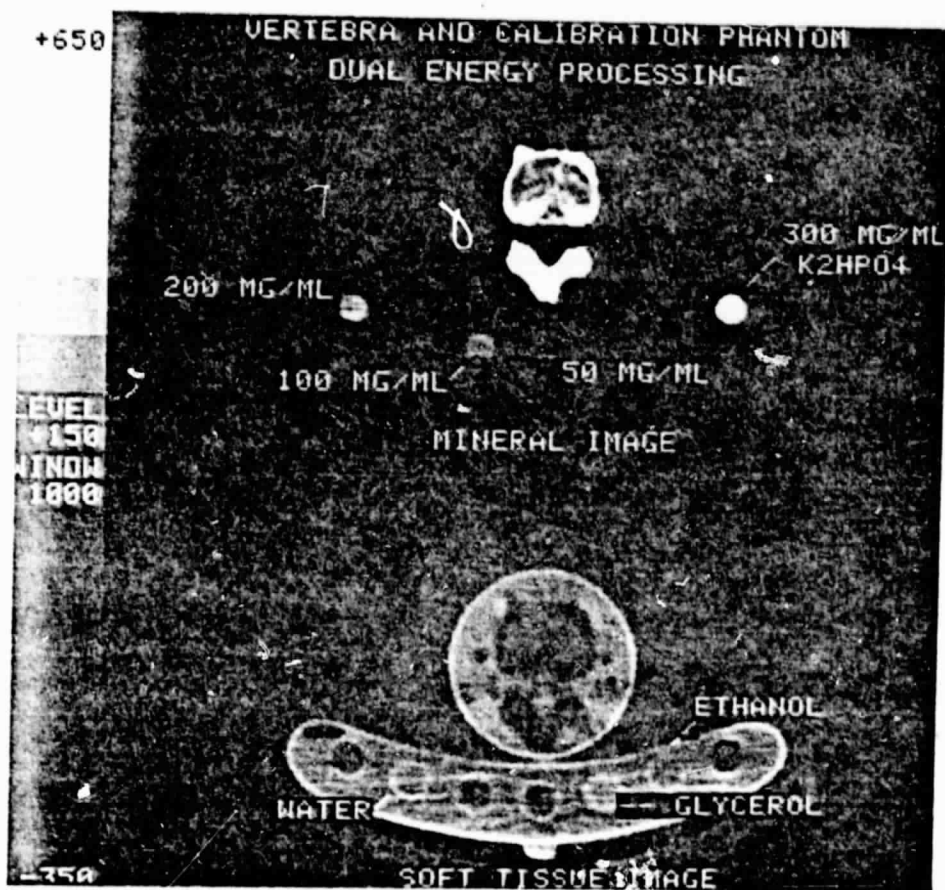and the amount of calcium in the spine.

Figure 3.   Images of mineral (aluminum) and soft tissue (plastic) distributions of an excised human vertebra and calibration phantom. Scans obtained at 80 kVp and 120 kVp and processed using energy-selective reconstruction techniques.

Theoretically, a system could be solved for a quantity such as c_1 if $\mu(E_1)$ and $\mu(E_2)$ could be measured directly and $\mu_1(E_1,E_2)$ were known. Unfortunately, the quantities $\mu(E_1)$ and $\mu(E_2)$ are never measured directly but are calculated from the non-linear set of measured attenuations $I/I_0 = e^{-\mu(E)x}$ along all rays passing through a particular point. Thus, a unique calculation of $\mu(E_1)$ and $\mu(E_2)$ is not possible based only on chemical composition at a particular point in the image, but must be based on the chemical composition at every point in the image. This restriction follows from the fact 1) that the attenuation of x-rays is a non-linear function of sample thickness because of the polychromaticity of the x-ray source, 2) the reconstruction operator is linear, and 3) these two operators do not commute.

There are two methods to approximate the true values for $\mu(E_1)$ and $\mu(E_2)$ under the conditions where the reconstructed image is available at E_1 and E_2. The first and most obvious method is to remove or reduce the polychromaticity of the source. This can be done by using monoenergetic radionuclide sources (6) or by selective filtration of the x-ray source. This will be addressed further in section C-1-c. The second method is to use iterative numerical techniques to produce a "corrected" image. This method has been attempted commercially (3) and some inaccuracies in the resulting CT numbers have been noted (7).

An alternative method for scanning with two different energy spectra has been used by Alvarez, Macovski and Avrin (8). In their method, it is important to notice that they do not reconstruct the energy-dependent linear attenuation coefficients. Instead, by explicitly considering the physics of x-ray interaction with substances of low to moderate atomic number they reconstruct the energy independent coefficients for the photoelectric effect and Compton scattering. There is difficulty for bone mineral determination in that the photoelectric image appears to be of low quality. In addition, the Compton and photoelectric images are not directly interpretable in biological terms. However, since the reconstructions are energy independent polychromatic errors do not arise directly. Based on the theory of Alvarez and Macovski, we have developed a preliminary method of bone mineral determination which produces a "soft tissue" image and a "mineral" image (Figure 3). For the preliminary result presented here, we used plastic (lucite) and very pure aluminum as the calibration materials. The images presented are, therefore, "plastic" and "aluminum" images. As explained in the following theoretical section, the choices of calibration materials are somewhat arbitrary and the results are interconvertible with other types of images such as water-hydroxyapatite.

The process of reconstruction of plastic-aluminum or other images which contain both Compton and photoelectric components is less noisy than pure Compton or photoelectric images. This is due to the more random nature of the noise in the plastic-aluminum image. The noise in Compton-photoelectric images is highly correlated and the numerical processing is also less stable.

The dual spectrum method differs in several major ways from other dual energy methods and from all single energy methods.

1) X-ray attenuation coefficients (or CT numbers) at the two equivalent energies are not reconstructed.

2) Typical density information is not used in a mixture rule, instead elemental composition data are used.

3) Some data processing is necessary on the original x-ray projection data taken by the scanner. Ordinary reconstructed images in CT numbers or attenuation coefficients cannot be used. This may require assistance from the scanner manufacturer to make the original data available for the computer program.

4) Variable overlying tissues or different amounts of fat in the spine do not directly cause errors. A thicker patient will reduce accuracy due to the decrease in photon flux available for measurement.

5) A calibration scan must be performed as often as necessary to correct for x-ray beam spectral drift. Small samples of known composition might be scanned with the patient to normalize minor drifts. The labor of recalibration is almost entirely dependent upon the particular scanner-computer system employed and the amount of automation that is possible.

b. Theoretical aspects of energy-selective reconstruction

For standard diagnostic x-ray spectra and the composition of the human body, the attenuation of x-rays by a particular small volume of material can be empirically approximated as

$$\mu(Z_i, \rho_i, c_i, E) = f_1(Z_i, \rho_i, c_i) \, g_1(E) + f_2(Z_i, \rho_i, c_i) g_2(E)$$

where f_1 and f_2 are functions of only the density and chemical composition of the volume element and g_1 and g_2 are functions of only the energy of the incident radiation. f_1 and f_2 can be represented as the Compton and photoelectric contributions to the material attenuation coefficient, respectively, or $f_1(Z, \rho, c) = \dfrac{\rho Z}{A}$, the average electron density and $f_2(Z, \rho, c) = \dfrac{\rho Z^n}{A}$, $n \sim 4$ empirically. f_2 is the empirical fit for the photoelectric effect for the energy range and elements considered.

g_1 is approximated by the Klein-Nishina function

$$g_1(E) = K_1 [1 - \frac{E}{510} + 5.2 \, (\frac{E}{510})^2] \text{ with E in keV and } K_1 \text{ an energy-}$$

independent fundamental constant.

g_2 is an empirical fit for the photoelectric function covering the energy range for all elements considered

$$g_2(E) = K_2/E^m, \quad m \sim 3$$

For the application considered here, material-selective image reconstruction, it is important that μ may be decomposed into the sum of products which each have a pure material-dependent factor and a pure energy-dependent factor. f_1 and f_2 are linear functions of the elemental concentrations in the mixture, that is

$$\frac{\partial f_1}{\partial c_i} = A_i \text{ for } i = Ca, P, O, \text{ etc.}$$

Thus, for any volume element a function f_1 can be defined in terms of its constant components f_1 (bone) and f_1 (soft tissue). In this basis set the attenuation for a volume located at a position x is

$$\mu(x, c_b, c_s) = [c_{cb}(x)f_{1,b} + c_s(x)f_{1,s}]g_1(E) + [c_b(x)f_{2,b} + c_s(x)f_{2,s}]g_2(E)$$

where $f_{i,j}$ are position-and energy-independent constants and c_b and c_s are the concentrations of bone and soft tissue, respectively, at position x.

Attenuation of x-ray spectra:

The photon flux at E from a source with peak energy E_1 is $S_1(E)$ and $S_2(E)$ for a source with peak energy E_2. S_1 and S_2 thus define the spectral distributions of sources with peak energies E_1 and E_2. The intensity transmitted along a line p is

$$I_1(p) = \int_{E=0}^{E_1} S_1(E) \ e^{-\int_p \mu(x,E)dx} \ dE$$

$$I_2(p) = \int_{E=0}^{E_2} S_2(E) e^{-\int_p \mu(x,E)dx} \ dE$$

in the bone/tissue basis set this is

$$I_1(p) = \int_{E=0}^{E_1} S_1(E) \{exp[(-f_{1,b}g_1(E)-f_{2,b}g_2(E))\int_p c_b(x)dx] \cdot$$

$$exp[(-f_{1,s}g_1(E)-f_{2,s}g_2(E))\int_p c_s(x)dx\}dE$$

and likewise for $I_2(p)$ and $S_2(E)$.

For a given series of experiments where $S_1(E)$ and $S_2(E)$ are constant spectra, $I_1(p)$ and $I_2(p)$ are functions only of the integrals of $c_b(x)$ and $c_s(x)$.

$$I_1(p) = H_1(\int_p c_b(x)dx, \int_p c_s(x)dx)$$

$$I_2(p) = H_2(\int_p c_b(x)dx, \int_p c_s(x)dx)$$

Direct measurement of $I_1(p)$ and $I_2(p)$ for various <u>combinations</u> of bone and soft tissue thicknesses can be done to calibrate the system, yielding

$$\int_p c_b(x)dx = Q_b(I_1(p), I_2(p))$$

$$\int_p c_s(x)dx = Q_s(I_1(p), I_2(p))$$

The functions Q_b and Q_s are empirically determined by curve fitting techniques. The integrals $\int c_b(x)dx$ and $\int c_s(x)dx$ are of the identical form as the attenuation integrals used to reconstruct the standard CT images. Therefore we can use existing reconstruction software and hardware to create images from these sets of integrals. We have converted our basis set, however, from x-ray attenuation to concentration of a particular chemical constituent. In this case, then, the images we display are not an image of x-ray attenuations but images of the distribution of mineral or soft tissue across the object, and our CT number scale corresponds to an absolute concentration scale.

The technique can be summarized as follows:

1) Scan the object with a spectrum of peak energy E_1 and obtain the values for $I_1(p)$ along all ray paths p. This is the original x-ray transmission data, or "raw" or "scan" data.

2) Scan with spectrum of peak energy E_2 to obtain $I_2(p)$.

3) Use the functions $Q_b(I_1,I_2)$ obtained from calibration data to calculate $\int_p c_b(x)dx$ and $\int_p c_s(x)dx$. These are the integrals of bone and soft tissue concentrations along ray path p.

4) Reconstruct the images using the functions $e^{-\mu_s \int_p c_s(x)dx}$ and $e^{-\mu_b \int_p c_b(x)dx}$. μ_s and μ_b are arbitrary constants to scale the data to fit the display system.

This method can be used to construct images of any two chemical components whose attenuation characteristics can be separated by judicious choice of scanning energies. Polychromaticity errors are eliminated as long as the x-ray spectra do not overlap K or L-shell edges of the elemental distribution being reconstructed (i.e. a gadolinium or silver-containing contrast material). For our purposes, bone mineral containing approximately 38% calcium and 19% phosphorus has significantly different attenuation characteristics than soft tissue composed of carbon, hydrogen, oxygen and nitrogen. The variable concentration of fat in the spinal bone mixture does not cause any error in the determination of mineral, because fat does not contain any "mineral" component in its attenuation characteristics.

RESULTS

The technique of dual energy reconstruction for spinal mineral measurement have been used to reconstruct independent "mineral" and "soft tissue" images for excised vertebral specimens (Figure 3). It can be seen in this figure that the calibration solutions containing mineral, as well as the spine, not only are present in the mineral image as they should be but are also absent in the soft tissue image. That is, these images represent the true physical situation in which mineral and soft tissue cannot physically occupy the same space. Results of quantitative analysis of these images are presented under Task 2.

TASK 2. To determine the relationship between measured attenuation coefticients and mineral content of the vertebral body.

The methods outlined in Task 1. have been used to generate mineral and soft tissue images of phantoms and excised vertebral specimens. Phantoms simulating the human torso and containing calibration materials (Figure 4) were scanned at 80 kVp and 120 kVp. The calibration materials are ethanol (fat-equivalent), glycerol (soft-tissue equivalent) and 50,100,200,300,400 mg K_2HPO_4/cm^3 (mineral-equivalent) solutions. The data for the mineral calibration curve obtained from the reconstructed "mineral" image is shown in Figure 5. The linearity (accuracy) of this data can be seen from the graph. Quantitatively, the dispersion about the regression line $(Sy/\bar{y})$ is 3.55%. This accuracy for the two-component calibration solutions compares quite favorably with previous measurements of two-component phantoms using single-energy CT (1), indicating that there are no systematic errors in the approach used for this energy-selective mineral-determination technique.

A total of 10 fresh excised human vertebrae have been obtained for this portion of the study. 3 of these have been scanned to determine mineral content, but because of the very limited availablity of human specimens they have not yet been destructively analyzed for mineral content. This procedure will be done when the dual-energy techniques have been perfected and calibrated using phantoms and mineral-equivalent solutions.
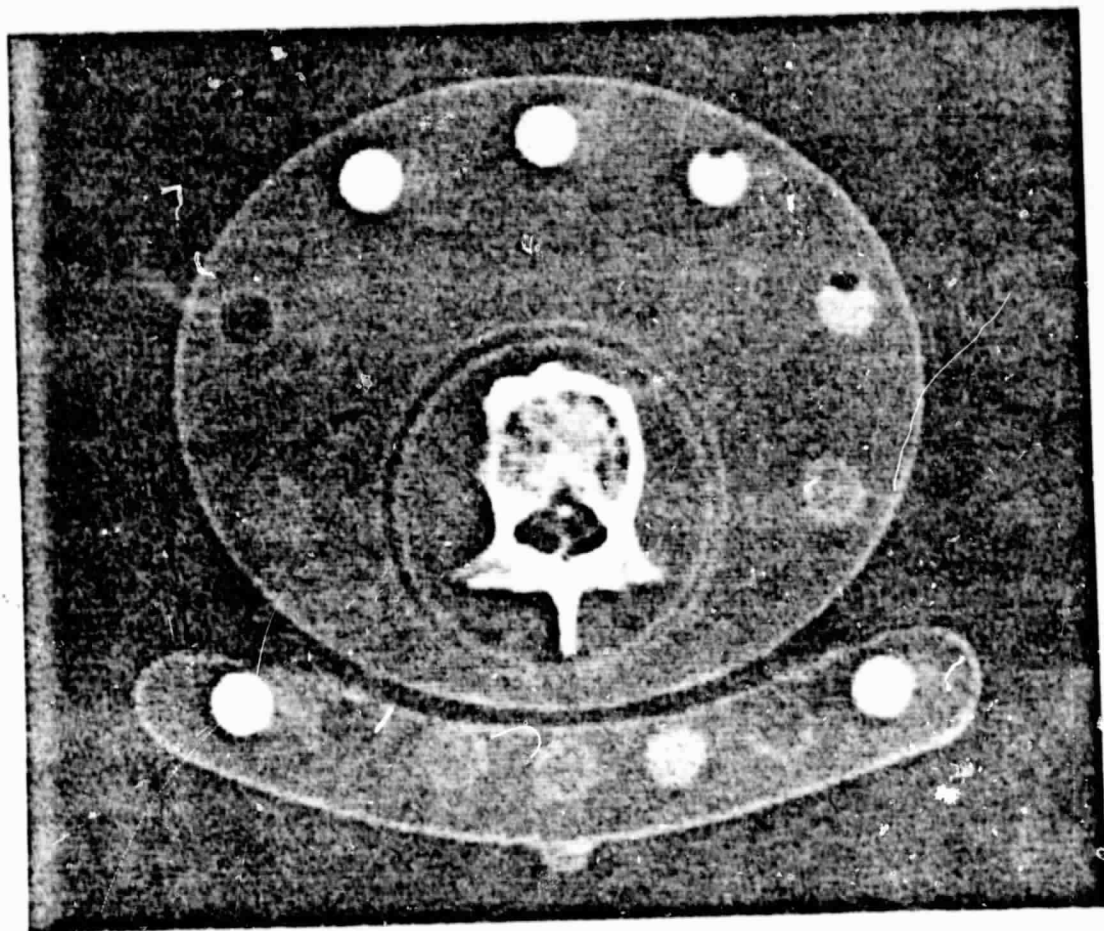
Figure 4.   CT scan of an excised vertebral specimen in a phantom simulating
the human torso. Cylindrical tubes contain calibration solutions
for mineral, soft tissue, and fat. Crescent shaped phantom under-
neath torso phantom is used for calibration purposes in all patient
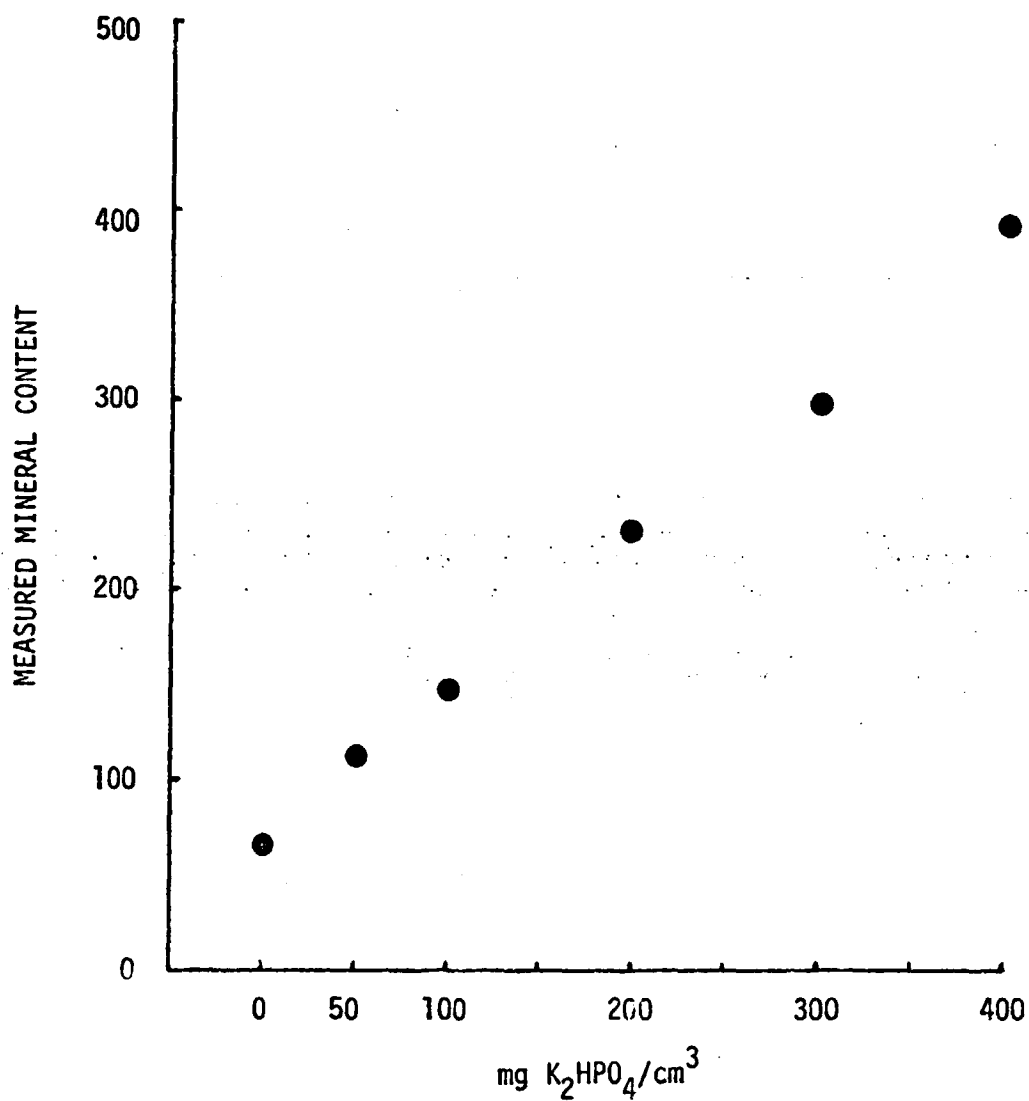studies.

Figure 5.   Relationship between mineral content measured using energy-selective reconstruction techniques and actual mineral content of calibration solutions containing K_2HPO_4. The slope of the line differs slightly from 1.00 because measured values are in terms of Aluminum-equivalent, and aluminum attenuates x-rays a bit differently than K_2HPO_4.

TASK 3. To construct specialized phantoms for vertebral mineral determination.

Phantoms simulating the human torso (Figure 4) and for patient calibration (Figure 6) have been constructed. One contains calibration materials fixed in position to scan with the patient for standardization purposes (Figure 6). The other is an outer phantom simulating a cross-section of the abdomen of approximately 65 cm circumference, and a removable center portion in which vertebral specimens or other calibration specimen materials can be inserted. 10 of these inserts have been constructed so that a large number of specimens can be scanned repeatedly, for example over a two week period, without having to remove them from their position within the insertable cylinder.

The initial calibration phantom used for dual energy technique development was a plastic step wedge with 15 steps combined with 5 varying thicknesses of high-purity aluminum. The dual-energy calibration method necessitates generation of a series of "constant plastic-variable aluminum" and "constant aluminum-variable plastic" curves which are solved using a set of orthonormal polynomials. Preliminary work with this phantom showed the feasibility of the methods; however, generation of a set of calibration data took 2 hours of scanner time and 16 hours of inter-active computer usage. Because the CT scanners used in this work may change slightly day-to-day or week-to-week, frequent recalibration would be necessary for clinical utility of the dual-energy scanning techniques and the time invested would be prohibitive. To solve this problem, a special phantom was constructed which allowed much more data to be obtained during a short scanning period. Computer programs specific for this phantom were written to read the data generated, analyze it, and generate the dual-energy calibration polynomials necessary for reconstruction of the mineral and soft tissue images. Total time for calibration purposes has now been reduced to approximately 20 minutes, so that this procedure can now be run routinely whenever a dual-energy scan of a patient is to be done.
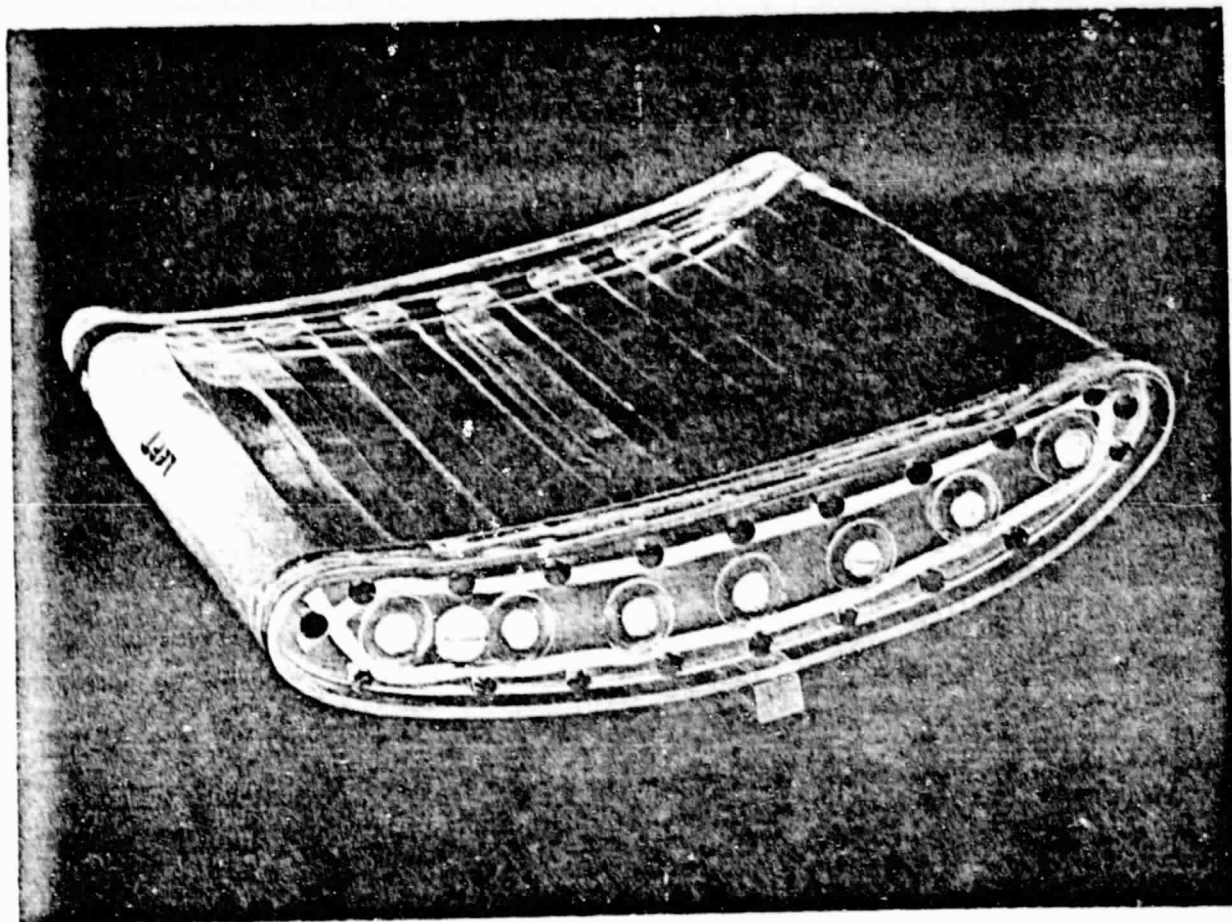
Figure 6.   Calibration phantom used for patient studies. Tubes contain varying
concentrations of K_2HPO_4, ethanol, glycerol and water to calibrate
for mineral, fat, and soft tissue at the same time the scan is done.

TASK 4. To determine vertebral mineral losses in serial studies in volunteer bedrest subjects.

Collaboration with Dr. V.S. Schneider, USPHS Hospital, San Francisco.

We use quantitative CT for vertebral mineral determination in a routine fashion for many of our clinical investigations. The techniques for precise serial measurements (9,10) have been developed over the last several years, and our in vivo coefficient of variation for normal, healthy adults is 1.54%. We used these techniques to measure vertebral mineral changes during 17 weeks of bedrest in normal adult male volunteers.

METHODS AND RESULTS

A total of 14 normal male volunteers, 20-44 years old, were recruited by Dr. Schneider for his studies of the effectiveness of dichloromethyldiphosphonate (Cl_2MDP) in the prevention of disuse osteoporosis. The study design included 12 weeks pre-bedrest equilibration and studies, 17 weeks of bedrest, and 3 weeks of post-bedrest follow-up. Some subjects were treated with Cl_2MDP and others were given a placebo. Treatment regimen was blinded to us until pre and post-bedrest vertebral measurements were made and the data analyzed.

Each volunteer subject was studied within 2 weeks prior to the start of bedrest and again within 1 week after the end of bedrest. No measurements were made during bedrest. The methods used have been described previously (9-11). Radiation dose for routine clinical measurements are 250mRem. For this study, doses were halved for a total radiation dose per study of 125mRem tightly coned to the region of L1 and L2. Multiple, contiguous non-overlapping 5 mm thick CT scans were obtained through the first and second lumbar vertebra at 80 kVp and 120 kVp, and the data were analyzed using special image processing software (Figure 7). Results are normalized to a calibration phantom scanned with the patient, and expressed as equivalent mg K_2HPO_4/cm^3. The results from the 14 subjects are presented in Table 1.

DISCUSSION

The aims of this study were three-fold: 1) to determine the magnitude of vertebral cancellous mineral loss in normal subjects during bedrest, 2) to compare this loss with calcium balance and mineral loss in periperal bones, and 3) to use the vertebral measurements as an evaluative criterion for the Cl_2MDP treatment and compare it with other methods.

The study design provided only 5 untreated individuals out of the total of 14 subjects. One of these individuals appeared to have a form of nutritional osteomalacia at the outset of the study and was in positive calcium balance for most of the study, correlating with his increase in vertebral mineral. The other 4 normal subjects showed changes of -9.2%, -9.3%, -12.2% and +3.1% (N.S.) of vertebral cancellous mineral during the 4 months of bedrest, or an average loss of 1.8% per month. This is a severe mineral loss from the spine and can be compared with our
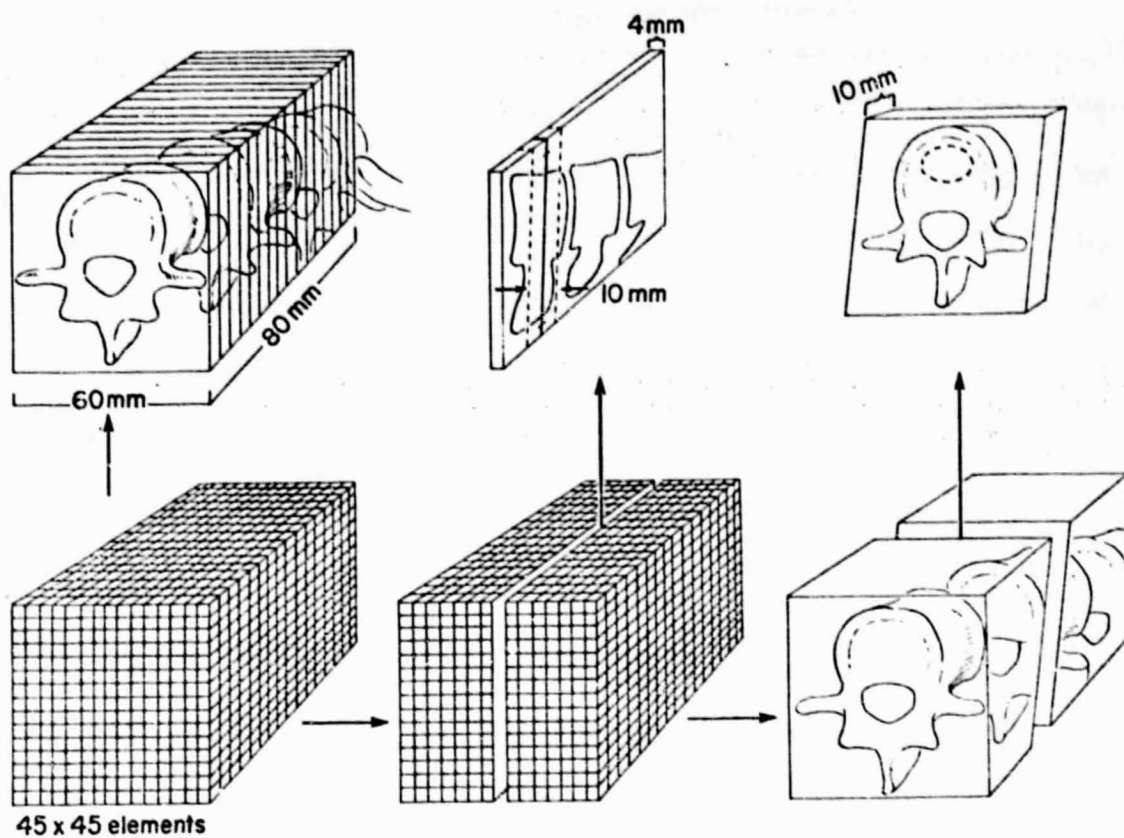
Figure 7. Illustration of the technique used to obtain precise positioning to the midportion of the lumbar vertebrae. Multiple contiguous axial scans are used to construct a volume containing the vertebrae. A single sagittal image is used to define a seven-pixel thick slice about the midplane of each vertebral body, and then this slice is synthesized from the data.

TABLE 1

Vertebral cancellous mineral change in 17 weeks of bedrest

Subject/Age		mineral (mg K_2HPO_4/cm^3)		% Change	Treated/ Untreated	Comment
		Pre-bedrest	Post-bedrest			
RF	43	154	140	-9.2	U	
MW	20	213	193	-9.3	U	
JD	28	176	166	-5.4	T	
RP	25	162	169	+4.2	T	
CC	23	147.4	160.7	+9.0	T	
PC	28	168.2	185.9	+10.5	T	
RV	27	175.6	177.2	+0.9	T	
RT	34	178.8	193.7	+8.3	U	Apparent initial Nutritional osteomalacia
DL	36	161.9	142.2	-12.2	U	
JH	24	168.8	175.1	+3.7	T	
FM	28	162.0	167.0	+3.1	U	
JSJ	30	147.1	152.1	+3.4	T	
RH	21	192.2	199.4	+3.7	T	
MR	27	169.4	174.2	+2.8	T	

maximal observed loss of 1.7% per month over a year in an oophorectomized women without replacement estrogen (10). These measurements of spinal loss in bedrest are the first data which document the postulated high rate of mineral loss from purely trabecular bone of the axial skeleton in the development of disuse osteoporosis. If, as has been hypothesized, bone loss during spaceflight is more severe than that seen in ground-based studies, we may expect to see a 3-5% per month loss of vertebral cancellous mineral. This may lead to clinical complications such as fracture or early osteoporosis for crew members of flights lasting 6 months or more.

The second aim of this study was to compare vertebral trabecular bone loss with mineral loss at other sites in the body (radius and calcaneus) and with total body calcium loss measured by balance techniques. The radial, calcaneal and balance measurements were made by Dr. V. Schneider at the USPHS Hospital. Complete data are not yet available for these correlation so results are not shown. They will be included in a later report.

The changes in vertebral mineral measured by the quantitative CT techniques were valuable in the evaluation of the drug treatment by providing an independent measure of bone loss in the axial skeleton. The precision of this technique was about 2.8% (CV) for the first 4 subjects, and improved to 1.6% for the later 10. Thus, a change of ~2 CV, or ~6% for early studies and 3-4% for the later studies would be interpreted as a significant change in vertebral cancellous mineral.

Four of the 5 untreated individuals lost an average of 6.9% over the 4 month bedrest period. The fourth subject was in strongly positive calcium balance in the equilibration period and positive balance for much of the bedrest portion of the study, indicating a "hungry bone" osteomalacic syndrome probably due to a calcium-deficient diet as part of this individual's normal nutritional status. This subject gained 8.3% in vertebral mineral during the course of the study.

The average change in vertebral mineral for the 9 treated subjects in this study was +3.6%. Statistical analysis for the treated vs untreated individuals using a t-test shows that the subjects treated with Cl_2MDP lost significantly less vertebral mineral (p<0.01) than the untreated subjects.

TASK 5. To determine the diagnostic potential for vertebral mineral determination in metabolic bone disease and in screening possible astronaut candidates (normal volunteers).

The primary emphasis of this task was to determine the normal vertebral cancellous mineral content in males and females and to compare mineral content in fracture patients with that in controls to determine if there is a vertebral fracture threshold. A total of 74 normal males and 93 normal females have been studied so far, in addition to 85 patients with various metabolic bone diseases. Of the patients, approximately 50 can be classed as osteoporotic or osteopenic of unknown etiology, while the others are grouped as hyperparathyroid, hemochromatosis, steroid osteoporosis and other diseases.

The results of vertebral mineral analyses in normal and osteoporotic subjects are shown in Figures 8 and 9. The data for normal individuals are grouped in 10-year intervals and the mean and 1 standard deviation for each age group are shown. The patients referred to us for clinical suspicion of osteoporosis are shown as filled circles.

Normal males start with a vertebral mineral density of approximately 190 mg cm^{-3} and lose a significant amount with aging, ~1.5% per year after age 50. This is in contrast to peripheral mineral measurements of cortical bone which show no loss with age for males in the radius and a slight loss from endosteal resorption in the metacarpals. Normal females have a similar pattern of vertebral mineral content with age, although the loss after age 45-50 appears to be somewhat greater than males, ~2-2.5% per year. Of particular interest may be the fact that females have the same vertebral density as males, ~180 mg cm^{-3}, before menopause, while peripheral bone mass is ~25% lower than for males. This appears to provide even more evidence that a measurement of peripheral mineral may not be useful in prediction of fracture susceptibility.

The large majority of patients referred to us as either osteoporotic or suspected osteopenic are female. For the most part the mineral content of these patients is below normal, although many fall within 1 standard deviation of the mean for their age. Those patients who have vertebral crush fractures tend to be among the lowest mineral values, but we do not yet have enough patients to identify a fracture threshold for vertebral cancellous mineral.
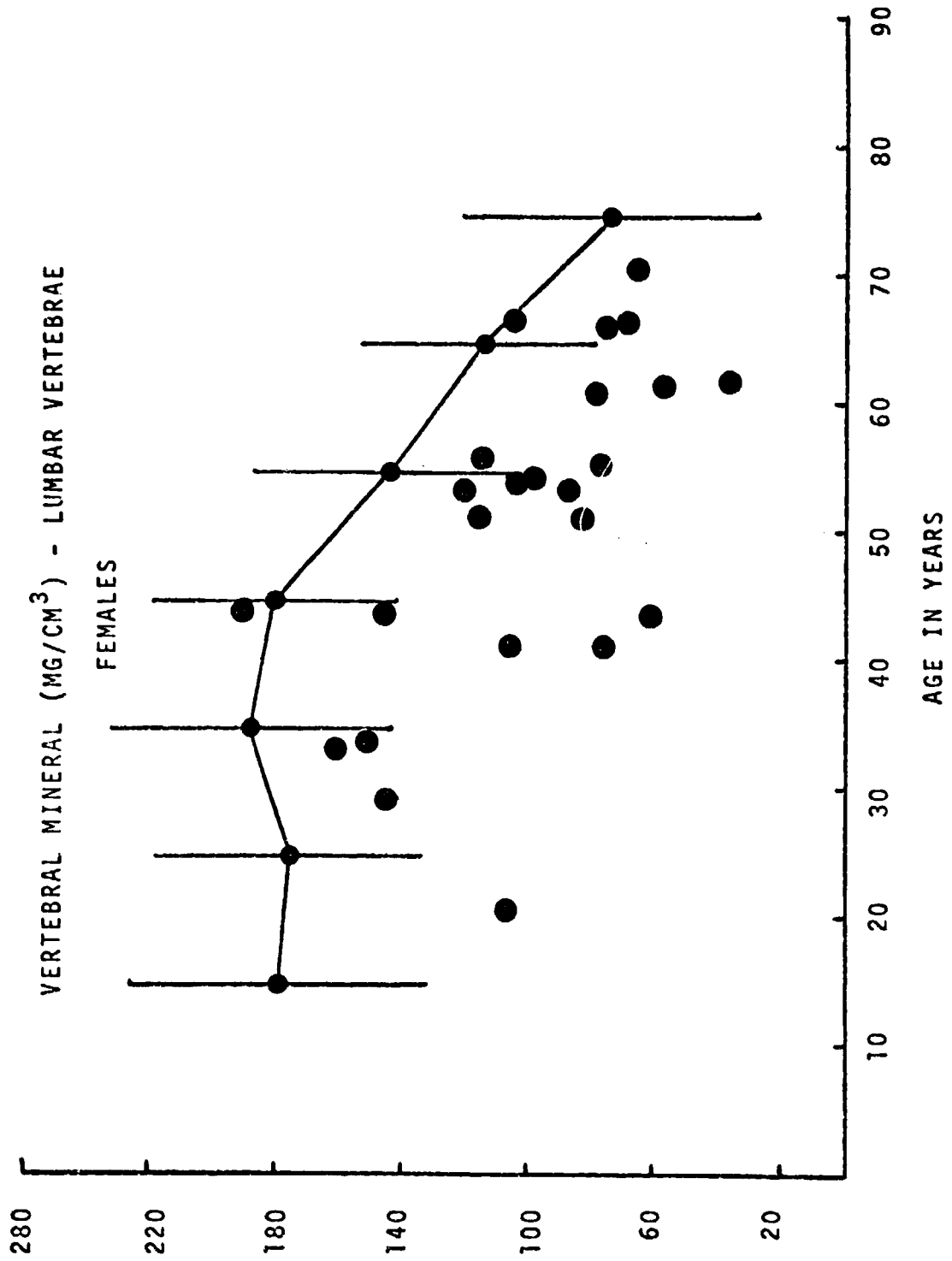
VERTEBRAL MINERAL (MG/CM^3) - LUMBAR VERTEBRAE

FEMALES

AGE IN YEARS

Figure 8.

VERTEBRAL MINERAL (MG/CM^3) - LUMBAR VERTEBRAE
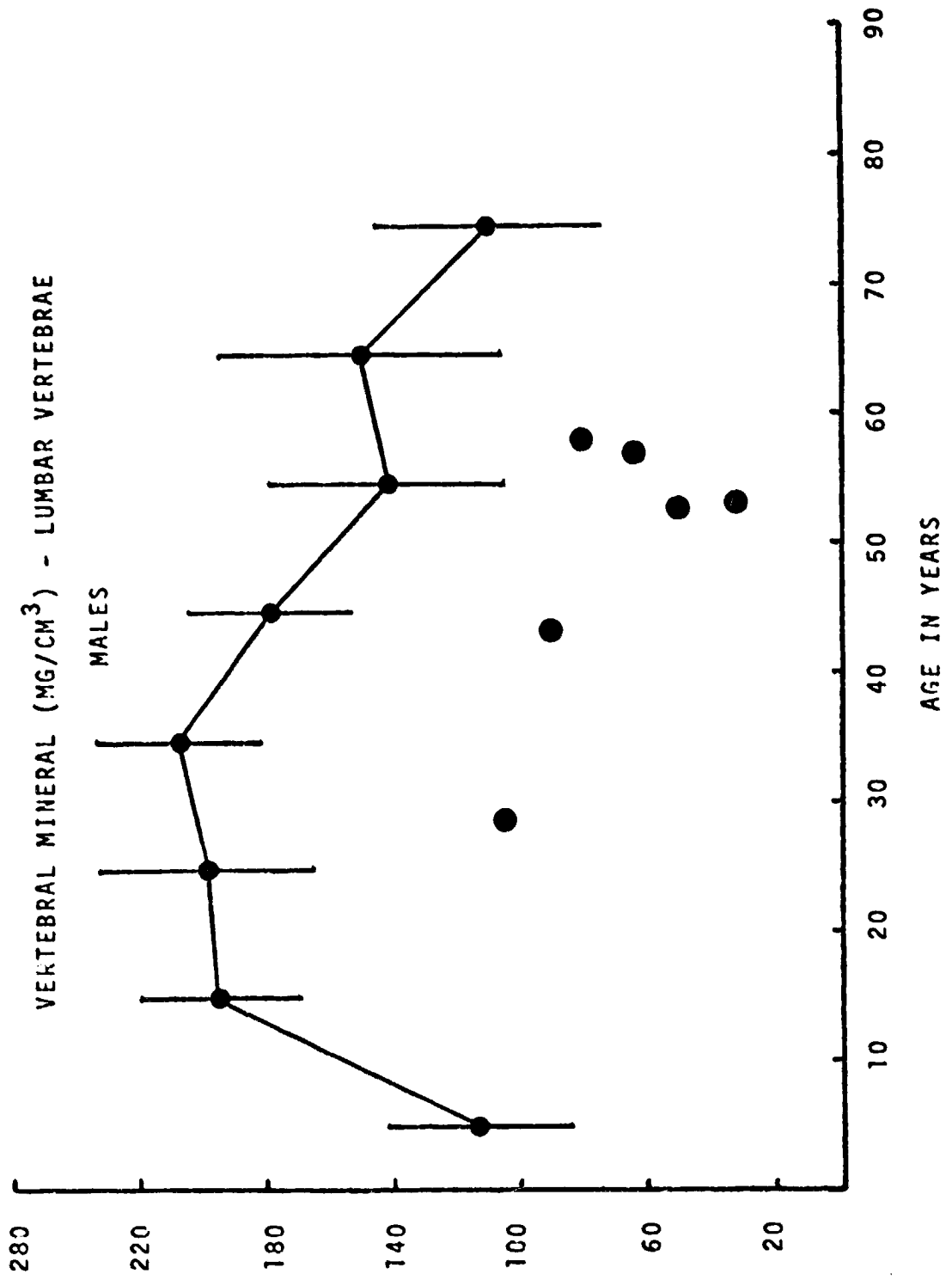
MALES

AGE IN YEARS

Figure 9.

REFERENCES

1. Genant HK, Boyd DP: Quantitative bone mineral analysis using dual energy computed tomography. Invest Radiol 12(6):545-551, 1977.

2. Rosenfeld D, Genant HK, Abols Y, Boyd DP: Analyses of multiple energy computed tomography techniques for the measurement of bone mineral content. In. Mazess (ed) Proceedings of the 4th International Conference of Bone Measurement, Washington, DC, US Government Printing Office, 1979.

3. Joseph PM, Spital RD: A method for correcting bone induced artifacts in computed tomography scanners. J Comput Assist Tomog 2:100-108, 1978.

4. Abols Y, Genant HK, Rosenfeld D, Boyd DP, Ettinger B, Gordan GS: Spinal bone mineral determination using computerized tomography in patients, controls and phantoms. In. Mazess (ed). Proceedings of the 4th International Conference on Bone Measurement, Washington, DC, US Government Printing Office, 1979.

5. Cann CE, Genant HK, Young DR: Comparison of vertebral and peripheral mineral losses in disuse osteoporosis in monkeys. Radiology 134:524-529, 1980.

6. Boyd DP: Computerized tomography: Isotope sources. Int J Radiation Oncol Biol Phys.3:43-56, 1977.

7. Joseph PM: Presented at First International Workshop on Bone and Soft Tissue Densitometry, San Francisco, CA, June 7-9, 1979.

8. Alvarez RE, Macovski A: Energy selective reconstructions in x-ray computerized tomography. Phys Med Biol 21:733-744, 1976.

9. Cann CE, Genant HK: Precise measurement of vertebral mineral content using computed tomography. J Comput Assist Tomog. 4(4):493-500, August 1980.

10. Cann CE, Genant HK, Ettinger B, Gordan GS: Spinal mineral loss by quantitative computed tomography in oophorectomized women. J Am Med Assoc. October, 1980, in press.

11. Cann CE, Genant HK, Boyd DP: Precise measurement of vertebral density changes in serial studies using computed tomography. Invest Radiology 14(5):372, Sept-Oct, 1979.